Extended Abstracts of the 2007 International Conference on Solid State Devices and Materials, Tsukuba, 2007, pp. 666-667

P-11-5

A Novel High-k Y_2O_3 Sensing Membrane for pH-ISFET

Tung-Ming Pan, Kao-Ming Liao, Jian-Chyi Lin, Chih-Hung Cheng, Zhao-Wen Lin, and Chih-Jen Chang
Department of Electronic Engineering, Chang Gung University,
259 Wen-Hwa 1st Road, Kwei-Shan, Tao-Yuan 333, Taiwan
Phone: +886-3-2118800 ext. 3349 E-mail: tmpan@mail.cgu.edu.tw

1. Introduction

Since Bergveld [1] reported on ion sensitive field effect transistors (ISFETs) for measuring ion concentrations in solutions, various kinds of chemical sensors have been developed which are based on Si semiconductor technology. In the literature relating to ISFETs, Bergveld's reported was cited as the first paper [2], many theoretical and experimental studies have been published to describe the behavior of this chemically sensitive electronic device. The commonly accepted model to account for the pH sensitivity of the ISFET is the site-dissociation model, which was firstly proposed by Yates et al. [3], and later applied to ISFETs by Siuand Cobbold [4] and Bousse [5]. Recently, high-k dielectric materials, such as Al_2O_3, Ta_2O_5, TiO_2, WO_3, and ZrO_2 [6-8] were proposed as hydrogen ion sensing membrane for pH-ISFET to replace Si_3N_4 membrane because of their high sensitivity performance. In this work, an yttrium oxide dielectric grown using reactive RF-sputtering was investigated as sensing membrane of pH-EIS structure.

2. Experiments

Before the deposition of Y_2O_3, the wafers were cleaned with a standard RCA. A 30-nm Y_2O_3 film was deposited by reactive RF sputtering. Samples were annealed by RTA at 700-900 ˚C for 30-s in N_2 gas. A 300-nm Al film was deposited on the backside of wafer by thermal evaporator. The sensing area was defined by a photosensitive epoxy, SU8-2005 in standard photolithography process. The processing flow and structure of EIS of Y_2O_3 sensing membrane were shown in Fig. 1. C-V curves of all samples for various pH buffer solutions (pH=2-12) were measured with substrate bias through Ag/AgCl reference electrode by HP4284A LCR meter.

3. Result and Discussions

Fig. 2 shows the XRD spectra of yttrium oxide film for as-deposited and annealed films. The as-deposited film is an amorphous and badly-crystallized structure, while the annealed film exhibits crystalline Y_2O_3 structure. Obviously, the sample annealed at 900 ^{o}C clearly depicts stronger peaks characteristic of (400) oriented Y_2O_3. Figs. 3-4 depict the XPS spectra of Y 3d and O 1s for Y_2O_3 sensing films before and after RTA treatment. For as-deposited samples, the Y $3d_{5/2}$ and Y $3d_{3/2}$ peak positions at 158.4 and 160.2 eV are consistent with the Y_2O_3 splitting reference position, respectively. The Y 3d binding energy peaks shift to high binding energy for sample after 900 ˚C annealing, indicating a high Si content in the Y-silicate. Furthermore, for samples annealed at 700 ˚C, the Y splitting peaks position at 158.4 and 160.2 eV and the O 1s position at 531 eV clearly indicate the presence of Y_2O_3 compound.

The typical C-V characteristics of Y_2O_3 EIS after annealing at 700 ˚C from the pH=2 to pH=12 buffer solutions were shown in Fig. 5. The C-V curves were shifted parallel with increasing hydrogen ion concentration to positive bias. This phenomenon can be explained by the surface site-binding model [3]. Fig. 6 demonstrates the pH sensing characteristics of the Y_2O_3 pH-EIS structure. It is clear that Y_2O_3 sensing film annealed at 700 ^{o}C has good linearity in a wide pH range (pH=2-12). Fig. 7 shows the sensitivity and drift for as-deposited film and film annealed different temperatures. The gate voltage drift of pH-ISFETs is modeled by using a hopping and/or trap-limited transport mechanism, to determine the rate of hydration of the gate insulator. The drift measurement was tested for 12 h. It is found the sample after RTA at 700 ˚C has a high pH-sensitivity of 53.8mV/pH and a small drift of 3.58mV/h, suggesting a well-crystallized Y_2O_3 structure and a small amount of Si content in the oxide. In contrast, the sample annealed at 900 °C exhibits a lower pH sensitivity and larger drift rate due to the presence of Y-silicate layer.

The sensor is directly to be immersed in pH=7→4→7→10→7 loops for 1500 s, in order to prevent the Y_2O_3 dielectric film dissolves in the solutions during the measuring processes. Fig. 8 depicts the gate voltage variation of Y_2O_3 sensing membrane with PDA at 700 °C during the pH=7→4→7→10→7 loops. Fig. 9 illustrates the hysteresis voltage of Y_2O_3 sensing membrane as a function of annealing temperature. Although EIS sensing film annealed at 800 °C has a lower hysteresis width, the formation of Y-silicate and SiO_x layer easily occurs during this annealing temperature. From the experimental results, the hysteresis voltage of Y_2O_3 gate EIS after annealing at 700 °C in N_2 ambient is 5.6 mV.

4. Conclusion

In this paper, we report thin yttrium oxide films with different annealing temperature. We find that the sample after RTA treatment at 700°C exhibit a larger sensitivity (53.8mV/pH), lower drift rate (3.58mV/h), and smaller hysteresis voltage (5.6 mV).

References

[1] P. Bergveld, IEEE Trans. Biomed. Eng. 17, 70, (1970).
[2] P. Bergveld, IEEE Trans. Biomed. Eng. 19, 342, (1972).
[3] D. E. Yates, et al., J. Chem. Soc., Faraday Trans., 70, 1807, (1974).
[4] W. M. Siu, et al., IEEE Trans. Electron Devices, 26, 1805, (1979).
[5] L. Bousse, Ph.D. Thesis, Enschede, (1982).
[6] D. H. Kwon, et al., Sen. Actuators B, 34, 441, (1996).
[7] J. C. Van Kerkhof, et al., Sen. Actuators B, 3, 129, (1991).
[8] S. Yoshida, et al., J. Electrochem. Soc., 151, H53, (2004).

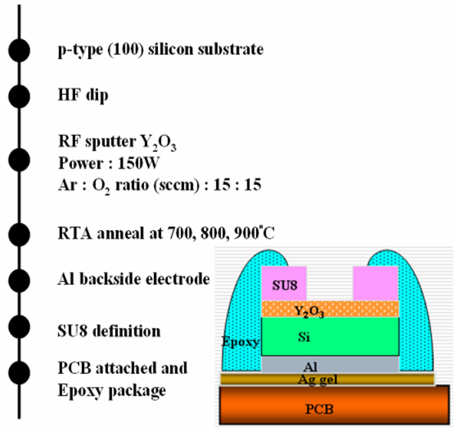

Fig. 1. The key processes flow and the Y_2O_3 film structure.

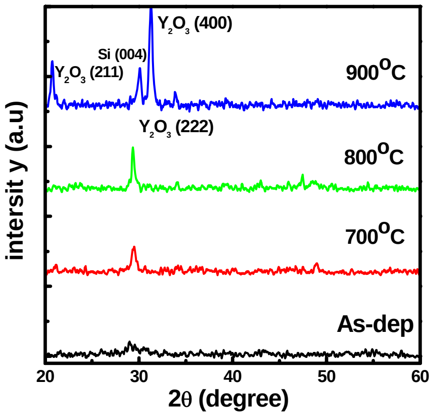

Fig. 2. XRD of Y_2O_3 film after different annealing temperatures.

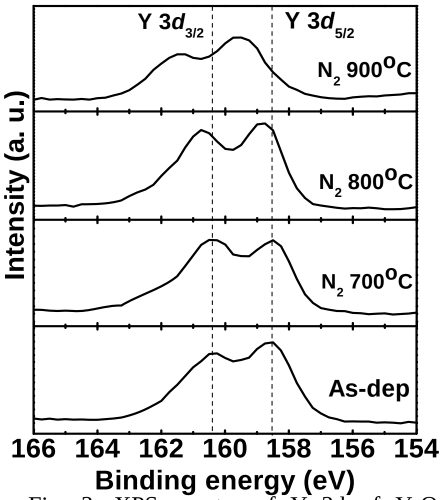

Fig. 3. XPS spectra of Y 3d of Y_2O_3 sensing films with different annealing temperatures.

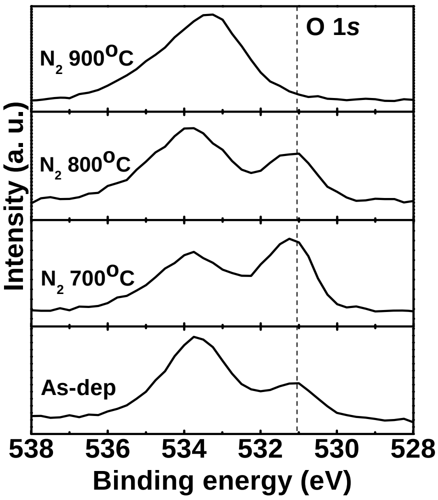

Fig. 4. XPS spectra of O 1s of Y_2O_3 sensing films with different annealing temperatures.

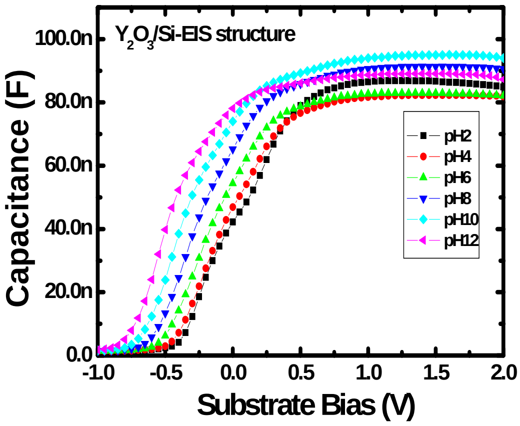

Fig. 5. Typical C-V curves of Y_2O_3 sensing film EIS immersing various pH solutions.

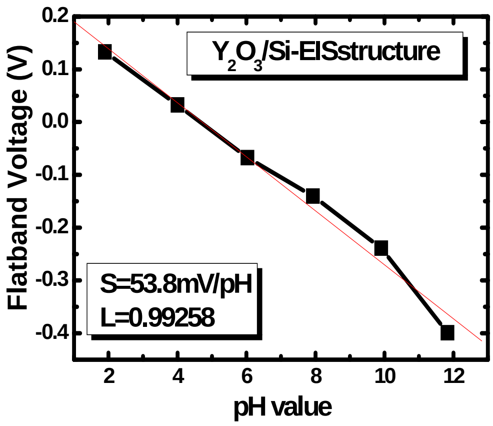

Fig. 6. Extracted response voltages as a function of various pH value for Y_2O_3 sensing film with fitting the sensitivity and linearity.

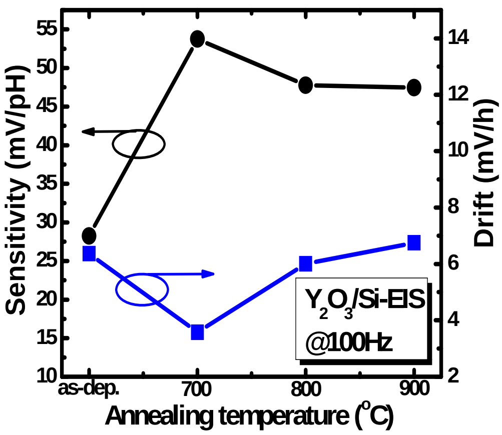

Fig. 7. Sensitivity and drift of Y_2O_3 layer after annealing various temperatures.

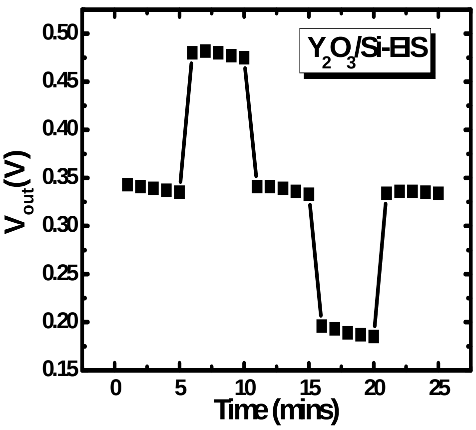

Fig. 8. A typical output voltage distribution of hysteresis measurement after annealing at 700°C in the pH=7→4→7→10→7 loops.

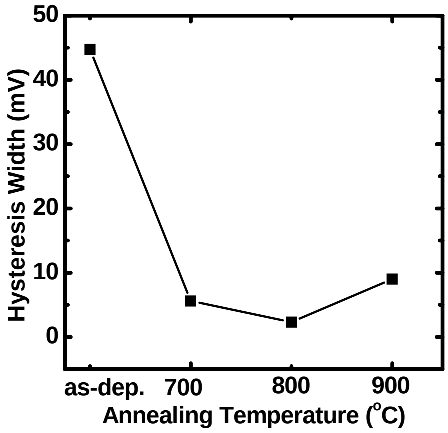

Fig. 9. Hysteresis width of Y_2O_3 sensing membrane with various RTA conditions.